



30th Eurosensors Conference, EUROSENSORS 2016

A monolithic silicon nanocrystal photonic transducer for a real-time biomarker detection

Chul Huh*, Jae Gab Lim, Wan-Joong Kim, Joo Yong Sim, and Bong-Kyu Kim

Bio-Medical IT Research Department, SW-Content Research Laboratory, Electronics and Telecommunications Research Institute, Daejeon 34129, Republic of Korea

Abstract

We demonstrate the monolithic Si nanocrystal (NC) photonic transducer for a real-time protein detection. The monolithic photonic transducer was composed of the Si NC light-emitting diode (LED), Si NC photodetector (PD), and Si nitride (SiN_x) optical waveguide that was optically self-aligned to the LED and PD. The Si NCs used as the fabrication of LED and PD were synthesized in the SiN_x matrix. Antibodies were immobilized onto the surface of SiN_x optical waveguide of the photonic transducer through self-assembled monolayers and surface aldehyde formation. Colloidal gold (Au) nanoparticles (NPs) were used to amplify the optical signal due to the strong surface plasmon resonance. The binding reaction of the Au NPs with the immobilized antibodies within the evanescent field at the transducer surface of the SiN_x optical waveguide causes attenuated total reflection of the waveguided modes and thus reduction of the PD photocurrent. The detection limit of prostate-specific antigen (PSA) was around 1 ng/mL.

© 2016 The Authors. Published by Elsevier Ltd. This is an open access article under the CC BY-NC-ND license (<http://creativecommons.org/licenses/by-nc-nd/4.0/>).

Peer-review under responsibility of the organizing committee of the 30th Eurosensors Conference

Keywords: Si nanocrystal; Photonic transducer; Optical waveguide; Au nanoparticle; Biomarker

1. Introduction

Because the photonic biosensors are immune to lots of interfering effects due to the noncontact nature between the analyte and transducer, they are superior to detect the biomarker (protein, DNA, enzyme, and cell) in body fluids (blood, sweat, urine, tear) compared to the electrochemical biosensor [1]. However, it is very difficult to reduce the cost and miniaturize the size of photonic biosensor since optical components (such as laser diode, scanner, and spectrometer) are relatively expensive and bulky. In order to overcome these obstacles, up to now, enormous researches have been done on searching for a highly efficient Si-based light source to realize the Si nanophotonics [2,3]. Especially, Si nanocrystal (NC) has attracted the most attention to realize the highly efficient light-emitting diodes (LEDs) due to a quantum confinement effect of Si NCs [4]. In our previous result [5], well-organized Si NCs

in the silicon nitride (SiN_x) film grown by a plasma enhanced chemical vapor deposition (PECVD) at a low temperature (250 °C) showed a clear quantum confinement effect depending on the size of Si NC, resulting that the band gap of Si NCs could be tuned from the near infrared (1.38 eV) to the ultraviolet (3.02 eV) range. In addition, we fabricated the mesa-type Si NC LED by applying an amorphous silicon carbide (SiC) film as an electron injection layer [6,7]. The results demonstrated that the electrons that stem from the amorphous SiC film could be effectively injected into the Si NC and subsequently recombine radiatively. In this work, we present a photonic biosensor based on a monolithic Si NC-based photonic transducer.

2. Experimental

The Si NCs used here were embedded into a SiN_x matrix with a thickness of 50 nm and were *in situ* grown by a conventional PECVD, in which Ar-diluted 10% SiH_4 and NH_3 was used as the source of reactants. The plasma power, chamber pressure, and substrate temperature for the growth of Si NCs were fixed at 6.8 W, 500 mTorr, and 250 °C, respectively. The size of Si NCs embedded into a SiN_x was around 4 nm, which was confirmed by a high-resolution transmission electron microscopy (HRTEM) [5]. No post annealing process was performed to create the Si NCs into the SiN_x matrix after the growth. An amorphous SiC film (approximately 45 nm) doped with P that is used as an electron injection layer was deposited on the Si NC layer at 300 °C by using a PECVD. Ar-diluted 10 % SiH_4 and CH_4 gases were employed to grow the n-SiC layer. A rapid thermal annealing (RTA) process at 950 °C for 2 min was performed to activate dopant sources into the SiC layer. After the RTA, the electron concentration of n-SiC layer was around $3 \times 10^{18} \text{ cm}^{-3}$. An ITO layer (100 nm) used as a transparent current spreading layer was deposited at RT on an amorphous SiC film by employing a RF sputter and then annealed at 600 °C for 1 min by using a rapid thermal annealing to improve the electrical property and optical transparency. Right after the deposition of ITO, the Si NC photonic transducer samples were etched using an inductively coupled SF_6/O_2 plasma and standard photolithographic technique until the Si layer was exposed. And then SiO_2 (around 2.5 μm) spacer layer was deposited and created by plasma etching. After spacer formation, the SiN_x optical waveguide with a thickness of 150 nm was deposited and lithographically patterned and etched in an inductively coupled SF_6/O_2 plasma. The thick SiO_2 spacer layer can minimize the substrate (Si) loss due to the difference in the dielectric constant between the SiO_2 and SiN_x containing the Si NCs. Finally, a Ni/Au (30/120 nm) layer was deposited for the top and backside contacts using thermal evaporation.

3. Results and Discussion

Figure 1 shows the fabricated monolithic Si NC photonic transducer. The photonic transducer integrates thin SiN_x optical waveguide along with self-aligned Si NC LEDs and Si NC PDs on a silicon chip. The sizes of Si NC LEDs are 100 $\mu\text{m} \times 200 \mu\text{m}$, 50 $\mu\text{m} \times 200 \mu\text{m}$, and 25 $\mu\text{m} \times 200 \mu\text{m}$, respectively. The sizes of Si NC PDs are 100 $\mu\text{m} \times 300 \mu\text{m}$, 50 $\mu\text{m} \times 300 \mu\text{m}$, and 25 $\mu\text{m} \times 300 \mu\text{m}$, respectively. The length and thickness of SiN_x optical waveguide are 2400 μm length and 150 nm, respectively. The width optical waveguide are 100, 50, and 25 μm , respectively. The sizes of photonic transducer are separated to optimize the optical coupling efficiency between the Si NC LED and Si NC PD through the SiN_x optical waveguide. The light emission from the Si NC LED with the size of 100 $\mu\text{m} \times 200 \mu\text{m}$ is shown in the inset of Fig. 1 (right and down side). As shown in the Fig. 1, the light emission from the Si NC LED was quite good and uniform. The light emitted from the Si NC LED upward enters the SiN_x optical waveguide and is guided to the Si NC PD. Efficient alignment and optical coupling of the Si NC LED and the Si NC PD with the integrated SiN_x optical waveguide were crucial to enhance the sensitivity of the monolithic photonic transducer for a biomarker detection. The Si NC LED-Si NC PD optical coupling efficiency calculated from the electrical and optical characteristics of these two devices was estimated to be 47 %.

Figure 2 shows the photocurrent obtained from Si NC PD as a function of the current injected into Si NC LED. As shown in the Fig. 2, with increasing the current applied to Si NC LED, the photocurrent from Si NC PD was nearly increased linearly. The photons injected from the Si NC LED was efficiently entered into the SiN_x optical waveguide and reached to the Si NC PD. From this result, it can be concluded that the Si NC LED was efficiently aligned with the Si NC PD through the SiN_x optical waveguide and also the Si NC LED-Si NC PD optical coupling efficiency was quite good.

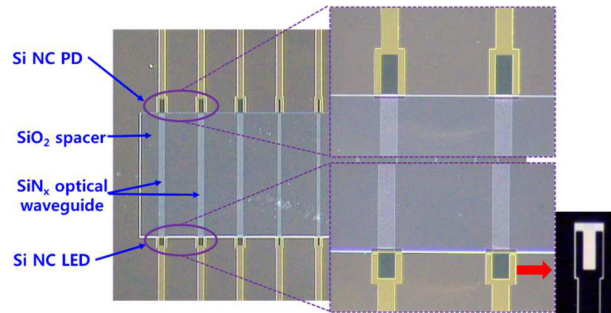


Fig. 1. A fabricated monolithic photonic transducer.

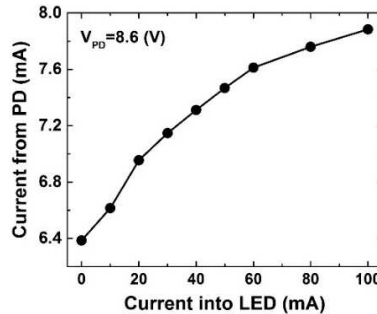


Fig. 2. A photocurrent obtained from Si NC PD as a function of the current injected into Si NC LED.

Because the sensitivity of a photonic transducer corresponds with antibody activity, it is very important to verify the density of the immobilized antibodies on the surface of SiN_x optical waveguide. The surface of SiN_x optical waveguide was treated by oxygen plasma to form hydroxyl groups (-OH) for chemical conjugation between the anti-prostate-specific antigen (PSA) and surface of SiN_x optical waveguide. Anti-PSA was immobilized onto surface of SiN_x optical waveguide through self-assembled monolayers (SAMs), surface aldehyde formation, and anti-PSA attachment sequentially. The conjugation method of Au NPs with a polyclonal antibody was described elsewhere in detail [8]. The surface of SiN_x optical waveguide immobilized with anti-PSA were immersed in the PSA antigen solution for 20 min at room temperature. Right after washing with a PBS solution, the sample was dipped into the solution containing Au NPs conjugated with polyclonal antibody for 1 h. And then, the sample washed out with the PBS solution and deionized water. Finally, the sample was dried with nitrogen gas. Figure 3 shows the FE-SEM images of Au NPs attached onto the surface of SiN_x optical waveguide. With increasing the PSA concentration, the number of Au NPs was increased. The numbers of Au NPs per μm² bound onto the surface of SiN_x optical waveguide for each concentration of PSA were (a) 1216 for 1 ng/mL, (b) 4096 for 50 ng/mL, and (c) 5504 for 100 ng/mL, respectively. As shown in Fig. 3(d), the number of Au NPs was proportional to PSA concentration, indicating that anti-PSA was efficiently immobilized onto the surface of SiN_x optical waveguide.

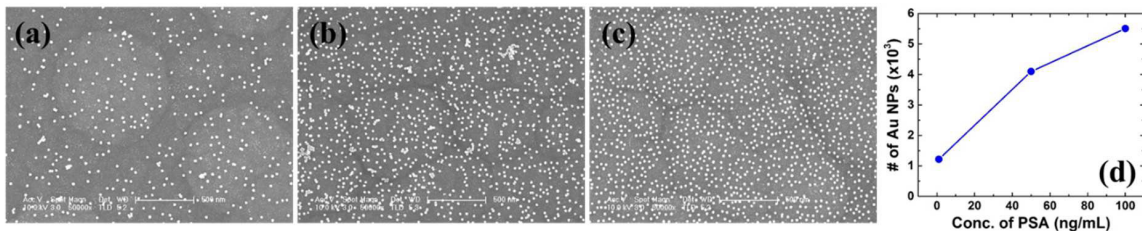


Fig. 3. FE-SEM images of Au NPs attached onto the surface of SiN_x optical waveguide.

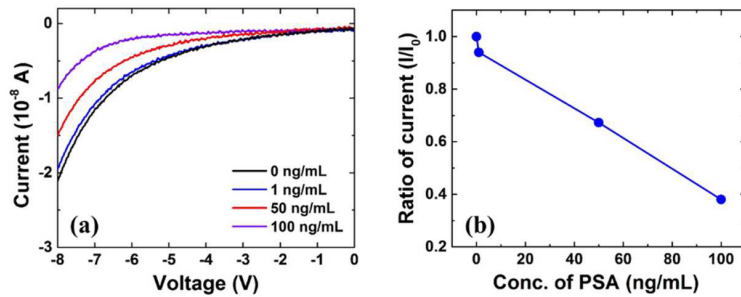


Fig. 4. (a) I-V curves of Si NC PD as a function of PSA concentration. (b) Ratio of current of Si NC PD as a function of PSA concentration.

Figure 4 shows (a) the I-V characteristics and (b) ratio of current of Si NC PD at a voltage of 8 V as a function of PSA concentration, respectively. As shown in Fig. 4(a), with increasing the PSA concentration, the current of Si NC PD was decreased. The number of Au NPs attached onto the surface of SiN_x optical waveguide was increased with increasing the PSA concentration. With increasing the Au NPs attached onto the surface of SiN_x optical waveguide, the optical coupling between the Au NPs and resonant mode of photons penetrating through the SiN_x optical waveguide was increased due to the strong surface plasmon resonance. Therefore, the reduction in the photocurrent of Si NC PD was attributed to an increase in the interaction between resonant mode photons penetrating through the optical waveguide and Au NPs attached onto the surface of optical waveguide and thus vanishment of photons traveling into the optical waveguide due to the scattering and absorption. As shown in Fig. 4(b), the photocurrent of Si NC PD was decreased by 60 %, when the concentration of PSA was increased up to 100 ng/mL. The result revealed a linear relationship within the range from 1 ng/mL to 100 ng/mL. We found that the PSA marker as low as 1 ng/mL could be detected by employing the monolithic Si NC photonic transducer.

4. Conclusions

In summary, a monolithic Si NC photonic transducer was presented. The transducer is based on the monolithic Si NC photocoupler consisted of the Si NC LED, Si NC PD, and SiN_x optical waveguide. In this photonic transducer, the signal transduction is attributed to the optical coupling deduction due to a strong surface plasmon resonance of Au NPs. The results show that the Si NC photonic transducer is capable of sensitive PSA detection in real time and also exhibits the advantages of photonic detection without the need of external photonic components.

Acknowledgements

This work was partially supported by Internal Research Program funded by the ETRI (16ZC1710).

References

- [1] A. P. F. Turner, Biosensors-Sense and sensitivity, *Science* 290 (2000) 1315-1317.
- [2] W. L. Ng, M. A. Lourenço, R. W. Gwilliam, S. Ledain, G. Shao, and K. P. Homewood, An efficient room-temperature silicon-based light-emitting diode, *Nature* 410 (2001) 192-194.
- [3] M. A. Green, J. Zhao, A. Wang, P. J. Reece, and M. Gal, Efficient silicon light-emitting diodes, *Nature* 412 (2001) 805-808.
- [4] L. Pavesi, L. Dal Negro, C. Mazzoleni, G. Franzò, and F. Priolo, Optical gain in silicon nanocrystals, *Nature* 408 (2000) 440-444.
- [5] T.-Y. Kim, N.-M. Park, K.-H. Kim, G. Y. Sung, Y.-W. Ok, T.-Y. Seong, and C.-J. Choi, Quantum confinement effect of silicon nanocrystals in situ grown in silicon nitride films, *Appl. Phys. Lett.* 85 (2004) 5355-5357.
- [6] C. Huh, K.-H. Kim, B. K. Kim, W. Kim, H. Ko, C.-J. Choi, and G. Y. Sung, Enhancement in light emission efficiency of a silicon nanocrystal light-emitting diode by multiple-luminescent structures, *Adv. Mater.* 22 (2010) 5058-5062.
- [7] C. Huh, B. K. Kim, C.-G. Ahn, C.-J. Choi, and S.-H. Kim, Enhancement in light emission and electrical efficiencies of a silicon nanocrystal light-emitting diode by indium tin oxide nanowires, *Appl. Phys. Lett.* 105 (2014) 031108-1~031108-4.
- [8] W.-J. Kim, B. K. Kim, A. Kim, C. Huh, C. S. Ah, K.-H. Kim, J. Hong, S. H. Park, S. Song, J. Song, and G. Y. Sung, Response to Cardiac Markers in Human Serum Analyzed by Guided-Mode Resonance Biosensor, *Anal. Chem.* 82 (2010) 9686-9693.